Journal of Hydrology: Regional Studies 40 (2022) 101023

Contents lists available at ScienceDirect

Journal of Hydrology: Regional Studies

journal homepage: www.elsevier.com/locate/ejrh

Evaluation of ERA5 and WFDE5 forcing data for hydrological modelling and the impact of bias correction with regional climatologies: A case study in the Danube River Basin

Elisabeth Probst *, Wolfram Mauser

Department of Geography, Ludwig-Maximilians-Universität München (LMU), Luisenstraße 37, 80333 Munich, Germany

ARTICLE INFO

Keywords:
Reanalysis
Precipitation climatology
Observational uncertainty
Alpine precipitation
WorldClim 2
PROMET

ABSTRACT

Study region: The Danube River Basin.
Study focus: Hydrological modelling of large, heterogeneous watersheds requires appropriate meteorological forcing data. The global meteorological reanalysis ERA5 and the global forcing dataset WFDE5 were evaluated for driving an uncalibrated setup of the mechanistic hydrological model PROMET (0.00833333°/1 h resolution) for the period 1980–2016. Different climatologies were used for linear bias correction of ERA5: the global WorldClim 2 temperature and precipitation climatologies and the regional GLOWA and PRISM Alpine precipitation climatologies. Simulations driven with the uncorrected ERA5 reanalysis, the WFDE5 forcing dataset, ERA5 bias-corrected with WorldClim 2 and ERA5 bias-corrected with a GLOWA-PRISM-WorldClim 2 mosaic were evaluated regarding percent bias of discharge and model efficiency.
New hydrological insights for the region: Simulations yielded good model efficiencies and low percent biases of discharge at selected gauges. Uncalibrated model efficiencies corresponded with previous hydrological modelling studies. ERA5 and WFDE5 were well suited to drive PROMET in the hydrologically complex Danube basin, but bias correction of precipitation was essential for ERA5. The ERA5-driven simulation bias-corrected with a GLOWA-PRISM-WorldClim 2 mosaic performed best. Bias correction with GLOWA and PRISM outperformed WorldClim 2 in the Alps due to more realistic small-scale Alpine precipitation patterns resulting from higher station densities. In mountainous terrain, we emphasize the need for regional high-resolution precipitation climatologies and recommend them for bias correction of precipitation rather than global datasets.

1. Introduction

Hydrological modelling is critically dependent on accurate meteorological forcing data. Observations from ground-based weather station networks are a very appropriate source of meteorological forcing data, but are often only available at the scale of smaller watersheds. However, hydrological modelling of large-scale watersheds covering hundreds of thousands of km^2 or more has gained increasing scientific interest. At this scale, international river basin organizations (IRBOs) have been established for most transboundary watersheds around the world, such as the International Commission for the Protection of the Danube River (ICPDR) for the

* Corresponding author.
E-mail address: elisabeth.probst@iggf.geo.uni-muenchen.de (E. Probst).

https://doi.org/10.1016/j.ejrh.2022.101023
Received 6 August 2021; Received in revised form 31 January 2022; Accepted 1 February 2022
Available online 21 February 2022

Danube River Basin (DRB). For instance, the IRBOs require scenario analyses of trade-offs between different management interventions regarding agriculture or water management in the context of climate change, biodiversity or aquatic ecology, for which hydrological modelling provides an indispensable contribution (Abbaspour et al., 2015; Döll et al., 2009; Malagó et al., 2017). However, when it comes to hydrological modelling of large-scale watersheds, continuous observation time series from weather station networks typically become sparse. Therefore, modelling studies have increasingly relied on high-resolution, gridded meteorological forcing datasets such as global reanalyses or regional climate models (RCMs) (e.g. Beck et al., 2017; Chen et al., 2018; Essou et al., 2017; Essou et al., 2016; Kay et al., 2015; Tarek et al., 2020). For example, the newly available global reanalysis ERA5 (Hersbach et al., 2020) and the global forcing dataset WFDE5 (Cucchi et al., 2020) deliver a global coverage with a spatial resolution of 0.25° and 0.5° and hourly temporal resolution. For most of the global land surface, these meteorological forcing datasets now approximate or surpass the spatial data density of available weather station networks, significantly facilitating hydrological modelling in data-scarce regions (Tarek et al., 2020). Even in well-equipped regions such as Central Europe, high-resolution meteorological forcing datasets approach the spatial density and temporal resolution of weather station networks. In Switzerland, for example, the weather station density corresponds to one station per 475 km^2 for temperature and one per 100 km^2 for precipitation (Gubler et al., 2017).

Moreover, a decline in operating ground-based weather stations has been observed in recent years in most countries around the world (Essou et al., 2016). The availability of global to regional high-resolution, gridded meteorological drivers offers great potential to compensate for this declining trend in observation data availability (Tarek et al., 2020), but still raises questions regarding their suitability for driving hydrological models, especially in large and complex watersheds. Being the successor to ERA-Interim (Dee et al., 2011), ERA5 benefits from a decade of developments in model physics, core dynamics and data assimilation (Hersbach et al., 2020) and should therefore outperform classical and even sophisticated interpolation of weather station network observations in terms of adequately describing atmospheric dynamics.

Nevertheless, global reanalyses often show systematic, regionally distributed biases compared to ground-based weather station observations – especially of precipitation – which has led to the development of bias correction methodologies (Muñoz-Sabater et al., 2021; Weedon et al., 2011). From a meteorological perspective, bias correction of reanalyses is widely considered an essential task to better reproduce spatial patterns of meteorological observations, but is nonetheless controversial for hydrological modelling purposes (Essou et al., 2016). The bias correction procedure is usually embedded in the downscaling routine of the gridded meteorological data, where complex sub-scale spatial characteristics of the meteorological parameters especially in mountainous terrain are incorporated (Shrestha et al., 2017). Interestingly, existing studies on the evaluation of bias correction routines have focused almost exclusively on different methods for bias correction (e.g. linear vs. quantile mapping) (Chen et al., 2013; Lafon et al., 2013) and have very rarely questioned the choice of appropriate reference observational data. First attempts of questioning the application-specific choice of reference datasets in the light of observational uncertainties have been undertaken by Prein and Gobiet (2017), Kotlarski et al. (2019) and Gampe et al. (2019), finding that observational uncertainties can be considerable depending on the reference dataset. Gampe et al. (2019) emphasized that considering multiple reference datasets for bias correction is highly important for obtaining robust results in climate change impact studies.

From a hydrological perspective, model calibration is widely perceived as another essential task to account for conceptualizations and aggregations of hydrological processes in the model description that are not fully physically described (Yilmaz et al., 2010). For this purpose, suitable model parameters are often determined by "trial-and-error" calibration of the hydrological model. Across the hydrological modelling community, great efforts are being undertaken to calibrate empirical and physically-based hydrological models down to the scale of smallest sub basins to maximize model efficiency (for the DRB, e.g. Pagliero et al., 2014 and Stagl and Hattermann, 2015). Such calibration efforts result in the best possible model fit over the chosen spatial and temporal model framework, but limit transferability over space and time, especially when considering, for example, climate change impact effects or – as in our case – comparing the suitability of different meteorological forcing datasets for hydrological modelling.

In this paper, we analysed the performance of the global meteorological reanalysis ERA5 and the global bias-adjusted forcing dataset WFDE5 for driving a physically-based hydrological model in a large, heterogeneous watershed and the possible improvements that could be achieved by linear temperature and precipitation bias correction of ERA5 with different global and regional reference climatologies. For this purpose, we applied different configurations for bias correction of ERA5 during the downscaling process. In a first step, no bias correction was applied at all. In a second step, different combinations of the global WorldClim 2 temperature and precipitation climatologies (Fick and Hijmans, 2017), the GLOWA Alpine precipitation climatology (Früh et al., 2006) and the PRISM Alpine precipitation climatology (Frei and Schär, 1998) were used as reference datasets for linear bias correction of temperature and precipitation. To ensure the best possible comparability between these different meteorological forcing datasets, the hydrological model was not calibrated with measured discharge and an identical model setup and parametrization was used for all simulation runs (ceteris paribus conditions).

We chose the large-scale DRB for a regional case study, which features very heterogeneous natural regions and hydrological characteristics comprising mountain ranges (Alps, Dinarides, Carpathians) and extended lowlands (Pannonian Basin, Romanian Plain). Due to its complexity, the DRB is a very appropriate pilot basin for a detailed analysis of the performance of global-scale meteorological forcing datasets for hydrological modelling and of the suitability of different reference datasets for bias correction under widely varying landscape conditions.

For our simulation studies, we used the mechanistic hydro-agroecological model PROMET (Mauser and Bach, 2009) at a spatial resolution of 30″ (0.00833333°). We performed four different long-term hydrological simulation runs (see Sect. 2.4) driven with the downscaled and optionally bias-corrected global meteorological reanalysis ERA5 and the downscaled global meteorological forcing dataset WFDE5 in the DRB for the period 1980–2016. First, we show a comparison of spatial patterns of long-term mean annual precipitation between the different downscaled meteorological forcing datasets and compare them with existing observation-derived

precipitation maps of the Danube. Second, we compare area averages of sub basin-specific long-term annual means of temperature, precipitation and evapotranspiration between the forcing datasets. Third, we evaluate the performance of the (optionally bias-corrected) global meteorological forcing datasets in terms of percent bias of discharge and model efficiency metrics for all simulation runs. Model efficiency metrics and percent bias of discharge were calculated from the comparison between modelled and observed daily discharge at selected sub basin gauges. Based on our results, we discuss the performance of the uncalibrated hydrological model in general, evaluate the suitability of the global meteorological datasets for driving a hydrological model in a larger watershed and discuss the importance of bias correction. In this context, we particularly highlight how the choice of different global to regional reference climatologies for bias correction of precipitation affected percent bias of discharge and model efficiency.

2. Materials and methods

2.1. The Danube River Basin

Shared by 20 countries, the DRB is the most international river basin in the world and the second largest river basin (~817,000 km^2) in Europe (Jungwirth et al., 2014). The Danube river drains wide parts of Central and South-eastern Europe and, as a waterway, connects very heterogeneous natural, cultural and economic regions (Jungwirth et al., 2014). The Danube originates in the Black Forest in south-western Germany and passes 10 countries to its mouth in the Black Sea. On its way, the Danube gradually changes its character from a mountain to a lowland river, crossing mountainous terrain along the eastern Alpine foothills as well as large basins like the Vienna Basin, the Pannonian Basin and the Romanian Plain (see Fig. 1). Hence, its watershed comprises very heterogeneous hydrological characteristics including mountain watersheds such as the Upper Danube, the Drava and the Sava basin and lowland watersheds such as the tributary basins of the Middle and Lower Danube. Linked to this, the DRB is commonly divided by mountain ranges into three main sections. The Upper Danube extends from its source to the Devín Gate in the Little Carpathians at the border of Austria and Slovakia (Jungwirth et al., 2014). The Middle Danube extends to the Iron Gate in the Carpathians at the border of Hungary and Romania and from here, the Lower Danube extends down to the mouth, including the Danube delta (Jungwirth et al., 2014).

In accordance with the heterogeneous topography, annual precipitation is very unevenly distributed throughout the Danube basin. In contrast to the "water towers" Alps and Dinarides with annual rainfall of up to 3200 mm/a in the Alpine high mountain range, the Lower Danube features rather dry lowland regions like the Pannonian Basin and the Romanian Plain, where annual rainfall amounts to 350 mm/a (Schiller et al., 2010). After 2857 river-km from source to mouth, the average discharge (MQ) of the Danube river at the outlet gauge in Ceatal Izmail amounts to 6550 m^3/s (Schiller et al., 2010).

2.2. The hydro-agroecological model PROMET

The physically-based hydro-agroecological model PROMET (Processes of Radiation, Mass and Energy Transfer) (Mauser and Bach, 2009; Mauser et al., 2015) models water, energy and carbon fluxes in an interlinked manner, strictly closing energy and mass balance on the land surface. PROMET simulates all processes in hourly time steps on a spatially distributed, raster-based architecture of custom spatial resolution. In this study, we chose to run PROMET on a 30″ grid (0.00833333° spatial resolution, ~1 km^2 at the equator) and with hourly temporal resolution. The model framework of PROMET comprises different components such as meteorology, soil, groundwater, vegetation, channel flow and agricultural management (with e.g. fertilization and irrigation options) modules, which are

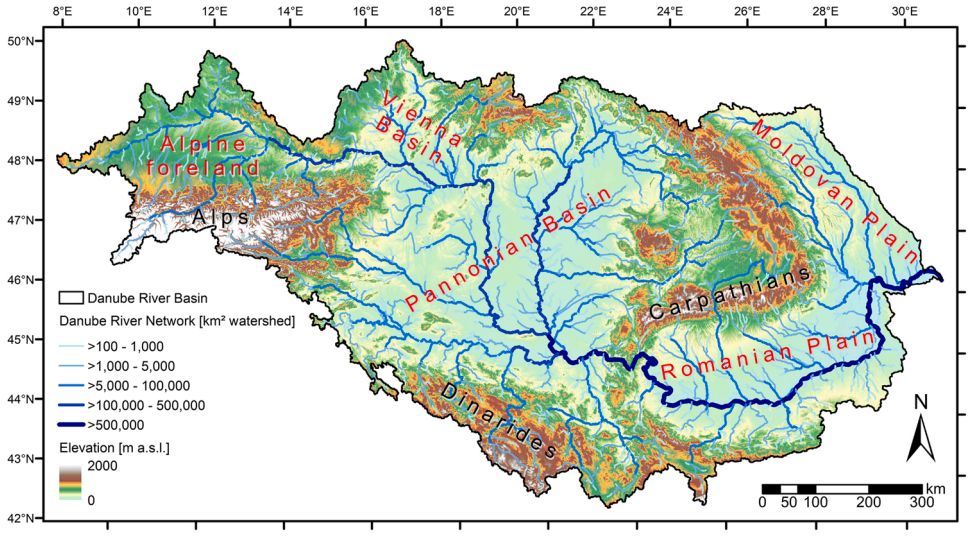

Fig. 1. Map of the Danube River Basin with its river network and major natural regions (data sources: Farr et al., 2007, Lehner et al., 2008).

described in detail in Mauser and Bach (2009), Hank et al. (2015), Mauser et al. (2015) and Zabel et al. (2014). The vegetation module simulates net primary production, land surface energy balance and evapotranspiration in an iterative manner using the mechanistic plant-physiology approach of Farquhar et al. (1980) and Chen et al. (1994), dynamically computing transpiration and CO_2 assimilation by C_3 and C_4 plant photosynthesis processes. Thereby a phenological component is triggered that uses trait information to simulate the weather-dependent annual development of 28 different plant types, representing various agricultural crops, pasture, forest and natural vegetation (see Sect. 2.5). The channel flow component calculates the channel routing of surface flow, interflow and baseflow through the river network to an outlet gauge following the approach of Muskingum-Cunge-Todini (Cunge, 1969; Todini, 2007). Due to its physical and physiological basis and spatial heterogeneity, a classical calibration of the PROMET model parameters to fit measured discharge is neither feasible nor desirable. Therefore, heterogeneous input parameters are used for watershed characterization (terrain, soil, land use, river width, channel slope and Manning coefficients) as well as for the system of linear storages, which receive percolation and are used to determine baseflow. The dynamical vegetation module is likewise supplied with consistent parameter sets for each plant type in the basin (see Sect. 2.5). In this study, PROMET was run with a comprehensive and plausibility-tested parametrization for hydrology and vegetation.

2.3. Meteorological downscaling and bias correction

The PROMET hydrological simulations are driven with gridded hourly time series of meteorological input parameters. Required parameters are air temperature (2 m height), total precipitation, air humidity (2 m height), surface air pressure, wind speed (2 m height), surface downwelling direct and diffuse shortwave solar radiation as well as surface downwelling longwave radiation. The PROMET meteorology module contains a routine that downscales and disaggregates coarse gridded meteorological forcing data to the custom spatial and temporal model resolution. In PROMET, a spatial downscaling approach is applied to the meteorological forcing data according to Marke et al. (2014) to bridge the gap between the coarse spatial resolution of the meteorological forcing datasets and the custom internal PROMET model resolution (30″ in this study). According to the approach of Marke et al. (2014), local elevation gradients are determined for elevation-dependent parameters and combined with the interpolation of de-trended residuals.

As part of the spatial downscaling routine, a spatially distributed, linear bias correction of hourly temperature and precipitation can optionally be applied. For this, PROMET applies spatially distributed daily patterns of bias correction coefficients to the downscaled meteorological forcing data to account for local biases in the meteorological parameters. Spatially distributed daily bias correction coefficients are derived from observed monthly climatologies of temperature and precipitation. For the linear bias correction, additive bias correction factors are used for temperature and multiplicative bias correction factors are used for precipitation. Bias correction of temperature is calculated following Eq. (1):

$$T_{corr,t} = T_{RAW,t} + f_{Tbias,d}, \tag{1}$$

where $T_{RAW,t}$ is the downscaled hourly temperature from the meteorological forcing data on a certain pixel, $f_{Tbias,d}$ the pixel-specific daily additive temperature correction factor and $T_{corr,t}$ the resulting bias-corrected hourly temperature value on the pixel. Bias correction of precipitation is calculated following Eq. (2):

$$P_{corr,t} = P_{RAW,t} * f_{Pbias,d}, \tag{2}$$

where $P_{RAW,t}$ is the downscaled hourly precipitation from the meteorological forcing data on a certain pixel, $f_{Pbias,d}$ the pixel-specific daily multiplicative precipitation correction factor and $P_{corr,t}$ the resulting bias-corrected hourly precipitation value on the pixel. Spatially distributed additive temperature correction factors are calculated following Eq. (3):

$$f_{Tbias,mon} = T_{CLIMmean,mon} - T_{RAWmean,mon}, \tag{3}$$

where $f_{Tbias,mon}$ is the pixel-specific monthly additive temperature correction factor, $T_{CLIMmean,mon}$ the long-term monthly mean temperature of the reference climatology on the pixel and $T_{RAWmean,mon}$ the long-term monthly mean temperature of the downscaled meteorological forcing data on the pixel. Spatially distributed multiplicative precipitation correction factors are calculated following Eq. (4):

$$f_{Pbias,mon} = P_{CLIMmean,mon} \quad / \quad P_{RAWmean,mon}, \tag{4}$$

where $f_{Pbias,mon}$ is the pixel-specific monthly multiplicative precipitation correction factor, $P_{CLIMmean,mon}$ the long-term monthly mean precipitation sum of the reference climatology on the pixel and $P_{RAWmean,mon}$ the long-term monthly mean precipitation sum of the downscaled meteorological forcing data on the pixel. In a last step, daily correction factors for temperature and precipitation are determined by a simple cubic interpolation of the monthly correction factors for each pixel.

2.4. Meteorological forcing data and climatologies for bias correction

For the hydrological modelling study in this paper, we used the ERA5 climate reanalysis produced by the European Centre for Medium-Range Weather Forecasts (ECMWF) and the derived bias-corrected WFDE5 forcing dataset as meteorological drivers. ERA5 is a global atmospheric, land and oceanic reanalysis calculated by the Integrated Forecasting System Cy41r2 (Hersbach et al., 2020). It is available from 1 January 1979 until present with a spatial resolution of 0.25° and hourly temporal resolution. WFDE5 is a global

forcing dataset directly based on ERA5, which is available from 1 January 1979 until 31 December 2018 on a spatial resolution of 0.5° and hourly temporal resolution. WFDE5 was derived from ERA5 surface meteorological variables, which were aggregated to 0.5° spatial resolution and some of them bias-corrected according to the WATCH Forcing Data (WFD) methodology (Cucchi et al., 2020; Weedon et al., 2011). For precipitation, bias correction is either based on the observed monthly Climate Research Unit Times Series version 4.03 (CRU TS4.03) (Harris et al., 2014) precipitation totals for 1979–2018 or on the observed monthly Global Precipitation Climatology Centre version 2018 (GPCCv2018) (Schneider et al., 2017) precipitation totals for 1979–2016 (Cucchi et al., 2020). Hence, WFDE5 precipitation is provided in a CRU-based and in a GPCC-based version (Cucchi et al., 2020). In this study, we used WFDE5 version 1.1 with GPCC-based precipitation. For the ERA5 and WFDE5 meteorological forcing datasets, it was necessary to apply a spatial downscaling procedure to comply with the PROMET model resolution of 30″ in this study (see Sect. 2.3). However, since both ERA5 and WFDE5 are available on hourly temporal resolution, no temporal disaggregation was necessary to comply with the hourly model time steps in PROMET.

To systematically determine the comparative skills of ERA5 and WFDE5 for driving PROMET, we used the downscaled ERA5 reanalysis as meteorological forcing for the hydrological simulations in different modifications: first, without any bias correction. Subsequently, we bias-corrected temperature and precipitation based on different global to regional reference climatologies. For this, we used the following temperature and precipitation reference climatologies:

- The global WorldClim 2 climatologies (Fick and Hijmans, 2017) of long-term mean monthly temperature and precipitation for the period 1970–2000 with a spatial resolution of 30″ (0.00833333°). The WorldClim 2 climatologies are based on 34,542 global weather stations from multiple sources (Fick and Hijmans, 2017).
- The regional PRISM climatology of long-term mean monthly precipitation covering the European Alps (Frei and Schär, 1998; Schwarb et al., 2001) for the period 1971–1990 with a spatial resolution of 2.5′ (0.04166666°). The PRISM climatology is based on more than 6600 rain gauge stations (Frei and Schär, 1998) and was thus created from a higher station density in the European Alps than WorldClim 2.
- The regional GLOWA climatology of long-term mean monthly precipitation covering the Upper Danube basin (Früh et al., 2006) for the period 1991–2000 with a spatial resolution of 30″ (0.00833333°). The GLOWA climatology is directly based on the PRISM climatology, which was transformed to the more recent reference period using 2198 weather stations (Früh et al., 2006).

For temperature, we created a single dataset of spatially distributed bias correction factors with a spatial resolution of 30″ according to Eq. (3). Here, we used long-term monthly mean temperatures of the WorldClim 2 reference climatology (1970–2000) and long-term monthly means of downscaled ERA5 temperature (1979–2000). For precipitation, we created two different datasets of spatially distributed bias correction factors with a spatial resolution of 30″ based on different combinations of precipitation correction factors derived from WorldClim 2, GLOWA and PRISM. According to Eq. (4), we used long-term monthly mean precipitation sums of the respective climatology (WorldClim 2, GLOWA or PRISM) and long-term monthly means of downscaled ERA5 precipitation sums for

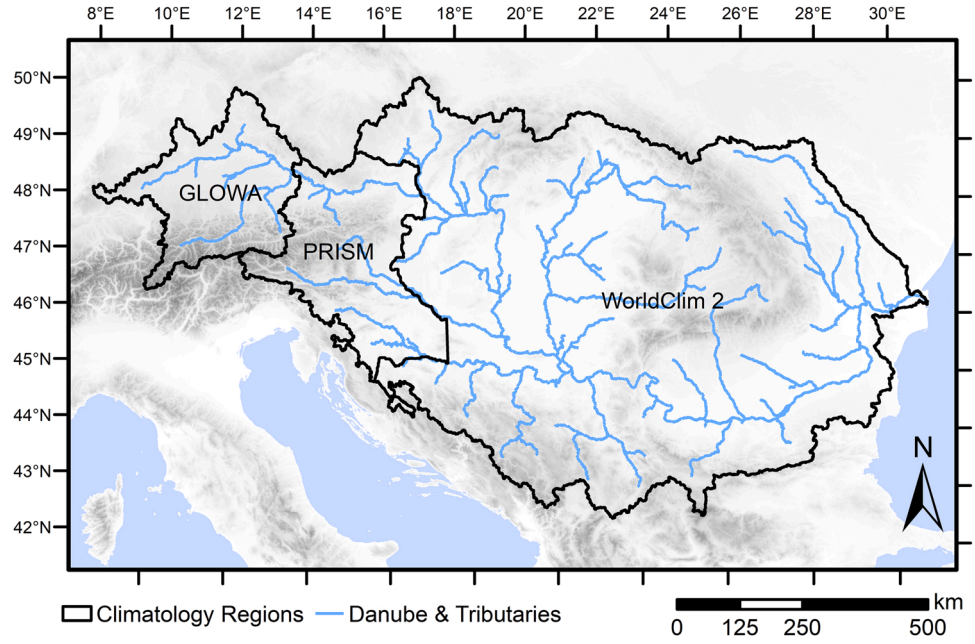

Fig. 2. Spatial coverage of precipitation climatologies within the Danube River Basin used to derive mosaicked spatial precipitation correction factors for bias correction of ERA5 resulting in the ERA5-GPW forcing dataset
(data sources: Lehner et al., 2008, Früh et al., 2006, Frei and Schär, 1998, Fick and Hijmans, 2017).

respective overlapping reference periods. For the WorldClim 2-derived precipitation bias correction factors, we took the ERA5 period 1979–2000, for the GLOWA-derived correction factors, we took the ERA5 period 1991–2000 and for the PRISM-derived correction factors, we took the ERA5 period 1979–1990. The two bias correction factor datasets for precipitation generated in this way consisted of:

- (i) the WorldClim 2-derived precipitation correction factors for the whole Danube basin. The meteorological forcing dataset consisting of ERA5 variables of which precipitation was bias-corrected with this precipitation correction dataset (and of which temperature was bias-corrected with the WorldClim 2-derived temperature correction factors) is further referred to as ERA5-WC in this paper,
- (ii) a mosaic of the GLOWA-derived precipitation correction factors for the Upper Danube basin, the PRISM-derived precipitation correction factors for the Alps and northern Dinarides outside the Upper Danube basin and the WorldClim 2-derived precipitation correction factors in the remaining Danube basin (see Fig. 2). The meteorological forcing dataset consisting of ERA5 variables of which precipitation was bias-corrected with this precipitation correction dataset (and of which temperature was bias-corrected with the WorldClim 2-derived temperature correction factors) is further referred to as ERA5-GPW in this paper.

In contrast to ERA5, we applied no additional bias correction to the downscaled WFDE5 product as it has already been bias-corrected according to the WFD methodology described in Cucchi et al. (2020) and Weedon et al. (2011). In this study, we therefore performed four different hydrological simulation runs in the DRB, each driven by one of the following meteorological forcing datasets: (i) ERA5, (ii) ERA5-WC, (iii) ERA5-GPW and (iv) WFDE5. In Table 1, we give an overview of the four different meteorological forcing datasets and global to regional datasets optionally used for bias correction of temperature and precipitation.

2.5. Model setup and gridded input data

PROMET used a digital terrain model derived from the global SRTM (Shuttle Radar Topography Mission) digital elevation model (Farr et al., 2007), in which radiometric slope and aspect was calculated from the SRTM elevation information. PROMET requires radiometric slope and aspect together with cloud cover from the meteorological forcing data to retrieve hourly direct and diffuse shortwave solar radiation components from the surface downwelling shortwave solar radiation. Soil properties data were derived from the Harmonized World Soil Database (HWSD) (FAO/IIASA/ISRIC/ISSCAS/JRC, 2012). Soil-specific sets of physical and hydraulic parameters were created for a four-layer soil column of 2 m depth following the approach of Brooks and Corey (1964). In mountainous terrain of $>$ 10% slope, we reduced total soil depth to 0.9 m. Watershed delineation, spatial flow direction and accumulation were derived from the global HydroSHEDS database (Lehner et al., 2008).

The land use map of the DRB used in this study is based on a mosaic of the CORINE Land Cover 2012 (European Environmental Agency (EEA), 2012) and the global ESA CCI Land Cover 2015 (European Space Agency (ESA), 2015). The CORINE Land Cover includes all EU member states within the DRB (i.e. Germany, Austria, Italy, Poland, Czech Republic, Slovakia, Hungary, Slovenia, Croatia, Romania and Bulgaria) as well as Switzerland and the non-EU Balkan states (i.e. Bosnia and Herzegovina, Serbia, Montenegro, Kosovo, North Macedonia and Albania). The ESA CCI Land Cover includes the territories of Ukraine and Moldova within the DRB that are missing in the CORINE Land Cover. The two land cover products provide detailed spatial information on a wide range of land cover categories, but lack information on the distribution of most agricultural crops (except for rice fields, vineyards, olive groves, fruits and berries, which are explicitly spatially distributed in the CORINE Land Cover). For hydrological modelling though, the proportional distribution of crops within sub basins is vital, because the modelled biophysical processes and water fluxes such as (evapo)transpiration are very crop-specific. To account for this, the PROMET dynamical vegetation module comprises several land use classes. They consist of 21 classes of agricultural crops (maize, winter/summer wheat, winter/summer barley, rye, oat, rapeseed, sunflower, soybean, silage, forage, hop, legumes, potato, sugar beet, rice, cotton, vegetables, fruits, set-aside), 2 pasture classes (extensive/intensive grassland) and 5 classes of natural vegetation (coniferous/deciduous forest, natural grassland, wetland, alpine vegetation). They are completed by 5 non-vegetative classes (rock, water, glacier, residential/industrial built-up). To create a land use map including the spatial distribution of agricultural crops, we consulted EU-wide and national statistics (EUROSTAT, 2013) on the cultivation area [ha]

Table 1
Overview of the meteorological forcing datasets and global to regional datasets optionally used for bias correction of temperature and precipitation (WFDE5 information according to Cucchi et al., 2020).

Meteorological forcing dataset	Datasets used for bias correction of temperature (T) and precipitation (P)	
	T	P
ERA5	None	None
ERA5-WC	WorldClim 2 temperature	WorldClim 2 precipitation
ERA5-GPW	WorldClim 2 temperature	GLOWA precipitation (Upper Danube), PRISM precipitation (Alps/Dinarides outside Upper Danube), WorldClim 2 precipitation (remaining Danube)
WFDE5	CRU TS4.03 temperature and diurnal temperature range	CRU TS4.03 number of wet days, GPCCv2018 precipitation totals

of the different crops per NUTS-II region for 2013 as reference year. Based on the cultivation statistics, we performed a spatially randomized distribution of agricultural crops over the agricultural land in the CORINE and the ESA CCI Land Cover within each NUTS-II region. In doing so, we did not attempt to achieve a completely spatially accurate distribution of agricultural crops (which is not even necessary due to crop rotation), but we developed a statistically correct representation of the proportional shares of crops on the agricultural land in each NUTS-II region. Comprehensive parameters for vegetation parametrization (sowing date, growing season, fertilization level) were derived from Sacks et al. (2010) and from agricultural crop yield statistics on country level (EUROSTAT, 2021).

2.6. Sub basin division and evaluation metrics

Considering long-term availability of discharge measurements, we divided the Danube basin into 8 sub basins (see Fig. 3), for which we analysed spatial precipitation patterns, area-averaged values for temperature, precipitation, evapotranspiration as well as percent bias of discharge and model efficiency based on modelled and observed daily discharge at the respective sub basin outlet gauges. Discharge measurements were obtained from the Global Runoff Data Centre (GRDC) (2019) and the International Commission for the Protection of the Danube River (ICPDR) (2021). Within the overlapping ERA5 and WFDE5 data availability period (1979–2018), daily discharge observations were available mainly for the period 1979–2016 (see Table 2). Thus, we performed the four different hydrological simulation runs driven by ERA5, ERA5-WC, ERA5-GPW and WFDE5 for the period 1980–2016, considering a decent model spin-up of 5 preceding years (1975–1979).

From the results of the four different hydrological simulation runs, we calculated the percent bias *PBIAS*[%] of the long-term daily discharge at the outlet gauges of the Danube basin and each of its sub basins according to Yapo et al. (1996) (Eq. (5)):

$$PBIAS = \frac{\sum_{t=1}^{T}(Q_{mod,t} - Q_{obs,t})}{\sum_{t=1}^{T}(Q_{obs,t})} * 100\% \,, \tag{5}$$

where $Q_{mod,t}$ stands for modelled discharge at time step t and $Q_{obs,t}$ for observed discharge at time step t. With PBIAS, we investigated whether the model correctly predicted the volume of modelled runoff or whether there was a potential tendency to over- or underestimate modelled discharge in the specific sub basins. We determined model efficiency based on Nash-Sutcliffe efficiency (NSE) and Kling-Gupta efficiency (KGE) of the daily discharge at the outlet gauges of the Danube basin and each of its sub basins. We calculated *NSE* according to Nash and Sutcliffe (1970) (Eq. (6)):

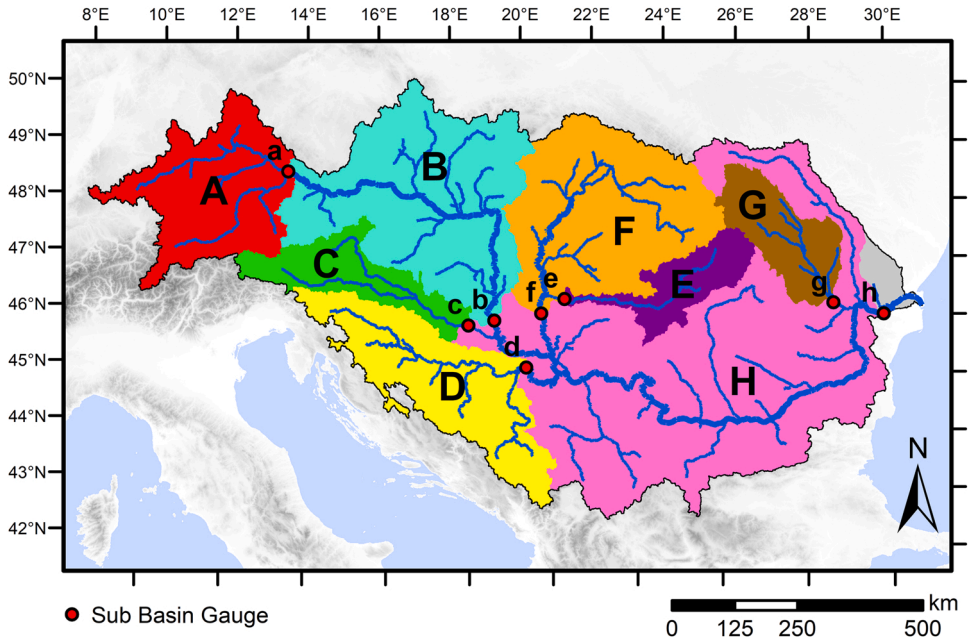

Fig. 3. Sub basin delineation within the Danube River Basin (A: Upper Danube, B: Middle Danube, C: Drava, D: Sava, E: Mures, F: Tisza, G: Siret, H: Lower Danube) and the corresponding outlet gauges (a: Achleiten, b: Bezdan, c: Dravaszabolcs, d: Sremska Mitrovica, e: Nagylak, f: Senta, g: Lungoci, h: Ceatal Izmail)
(data sources: Global Runoff Data Centre (GRDC), 2019; International Commission for the Protection of the Danube River (ICPDR), 2021; Lehner et al., 2008).

Table 2
Overview of the Danube sub basins and the corresponding outlet gauges with data source and availability of daily discharge measurements.

ID (Fig. 3)	Sub basin	Gauge	Data source	Daily discharge data availability for 1979–2018
A	Upper Danube	Achleiten (DE)	GRDC	1979–2015
A and B	Upper + Middle Danube	Bezdan (RS)	GRDC	1992–2010
C	Drava	Dravaszabolcs (HU)	ICPDR	1998–2000; 2002–2016
D	Sava	Sremska Mitrovica (RS)	GRDC	1992–2010
E	Mures	Nagylak (HU)	ICPDR	2007–2009; 2011–2016
F	Tisza	Senta (RS)	GRDC	1979–2010
G	Siret	Lungoci (RO)	GRDC	1979–2010
A to H	Danube overall	Ceatal Izmail (RO)	GRDC	1979–1995; 1997–2010

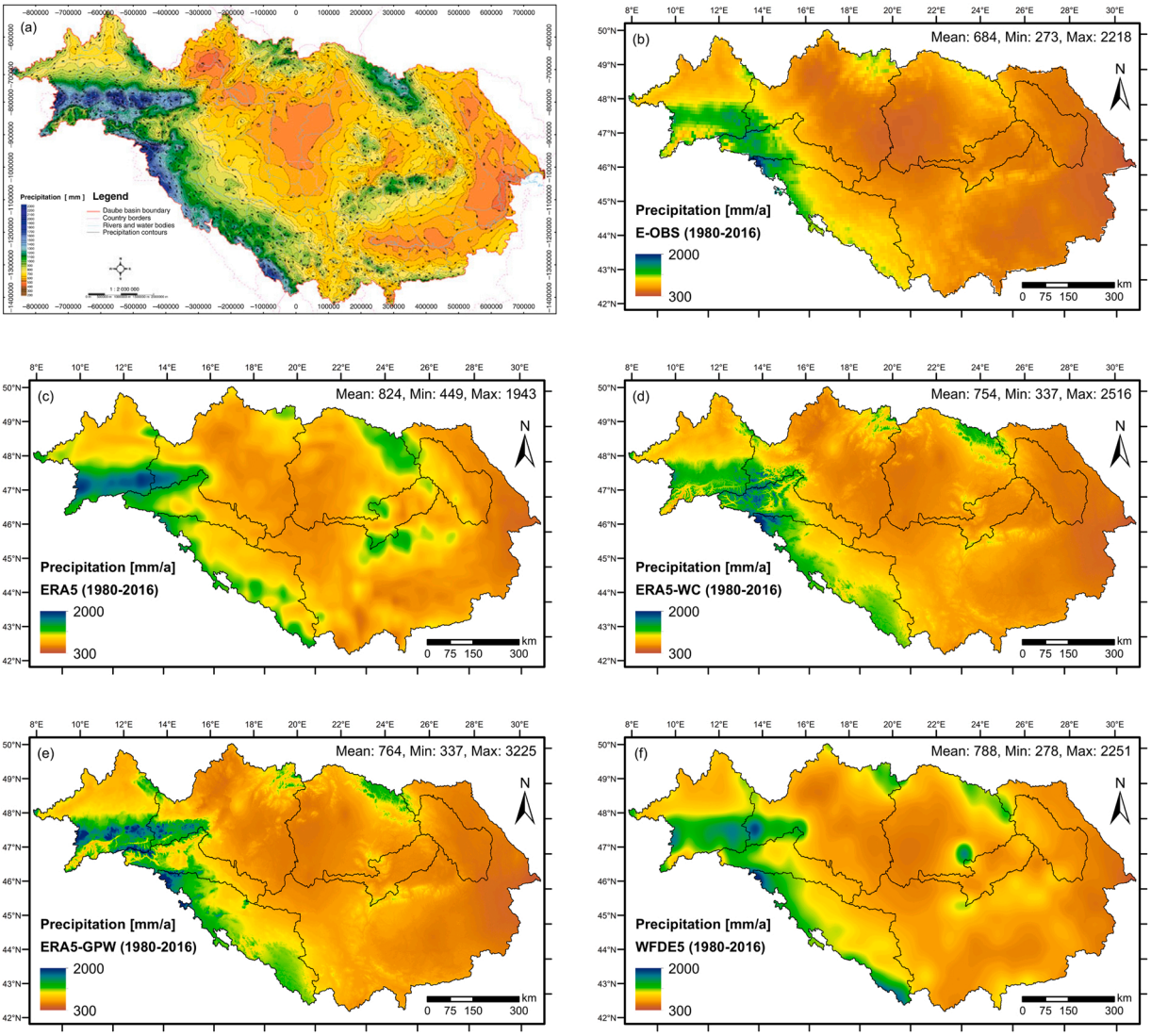

Fig. 4. Map of long-term annual mean precipitation [mm/a] in the Danube basin from interpolated observations for the period 1961–1990 created by the Institute of Hydrology at the Slovak Academy of Sciences (SAS) (Kovács, 2010; Petrovič et al., 2010). Adapted by permission from Springer Nature Customer Service Centre GmbH: Springer Nature, Characterization of the Runoff Regime and Its Stability in the Danube Catchment by P. Kovács, In: Brilly, M. (Ed.), Hydrological Processes of the Danube River Basin. © Springer Science+Business Media B.V. (2010) (https://doi.org/10.1007/978-90-481-3423-6_5). All rights in Fig. 4a are owned by Springer Nature; permission for any further reuse must be obtained from Springer Nature (a). Maps of long-term annual mean precipitation [mm/a] in the Danube basin for the period 1980–2016 from the E-OBS gridded precipitation observation product (v22.0e, 0.1°) (Cornes et al., 2018) (b) and from the downscaled forcing datasets ERA5 (c), ERA5-WC (d), ERA5-GPW (e) and WFDE5 (f).

$$NSE = 1 - \frac{\sum_{t=1}^{T} (Q_{mod,t} - Q_{obs,t})^2}{\sum_{t=1}^{T} (Q_{obs,t} - \overline{Q_{obs}})^2}, \quad (6)$$

where $Q_{mod,t}$ is the modelled discharge at time step t, $Q_{obs,t}$ is the observed discharge at time step t and $\overline{Q_{obs}}$ is the mean of observed discharges. We calculated *KGE* according to Gupta et al. (2009) and Kling et al. (2012) (Eq. (7)):

$$KGE = 1 - \sqrt{(r-1)^2 + (\frac{\mu_{mod}}{\mu_{obs}} - 1)^2 + (\frac{\sigma_{mod}/\mu_{mod}}{\sigma_{obs}/\mu_{obs}} - 1)^2}, \quad (7)$$

where r is the correlation coefficient between modelled and observed discharge, μ_{mod} is the mean modelled discharge, μ_{obs} is the mean observed discharge, σ_{mod} is the standard deviation of modelled discharge and σ_{obs} is the standard deviation of observed discharge. The KGE metric is widely perceived as a significant improvement to NSE and can be understood as a decomposition of NSE into its components, which measure the linear correlation, the bias and the variability of flow (Gupta et al., 2009). Nevertheless, both metrics have very specific strengths and weaknesses and cannot be directly compared to each other (Knoben et al., 2019). NSE = 1 and KGE = 1 indicate perfect agreement between model and observations, NSE = 0 and KGE = −0.41 indicate that the model has the same explanatory power as the mean of the observations and NSE < 0 and KGE < −0.41 indicate that the model is a worse predictor than the mean of the observations (Knoben et al., 2019).

3. Results

3.1. Spatial precipitation patterns

A realistic representation of spatial precipitation patterns in the meteorological forcing data is crucial for successful hydrological modelling, as rainfall distribution strongly influences the dynamics of runoff formation within a watershed and the timing and potential coincidence of flood waves at the confluences of rivers. It is important to note that spatial precipitation patterns from interpolated observations are strongly dependent on the underlying interpolation methods. Interestingly, we found that precipitation patterns differ greatly in various precipitation maps of the Danube available in the literature. Fig. 4 depicts a comparison of different maps showing observed precipitation from various sources as well as downscaled precipitation from our meteorological forcing datasets. We show long-term annual mean precipitation from interpolated observations for the period 1961–1990 created by the Institute of Hydrology at the Slovak Academy of Sciences (Kovács, 2010; Petrovič et al., 2010) (in the following denoted as SAS map) (a). Moreover, we show long-term annual mean precipitation from the E-OBS gridded precipitation observation product (version 22.0e, ensemble mean, 0.1° spatial resolution) for the period 1980–2016 (Cornes et al., 2018) (b). Furthermore, we show long-term annual mean downscaled precipitation for the period 1980–2016 from our forcing datasets ERA5 (c), ERA5-WC (d), ERA5-GPW (e) and WFDE5 (f).

Apparently, there are large differences in precipitation patterns visible between the two observation maps, especially in mountain regions like the Alps, the Dinarides and the Carpathians. Particularly striking is that the SAS precipitation map (a) shows a distinct rainfall band in the Bavarian Alpine foreland (extending far to the east), which is far less pronounced in the E-OBS precipitation map (b). The SAS map moreover shows a round-shaped dry region in the south-eastern (Slovenian) Alps, which is not present in the E-OBS map. In the SAS map, precipitation ranges from ~200 mm/a near the Danube delta to ~2300 mm/a in the Alpine foreland close to the Northern Limestone Alps and around the Dinaric mountain peaks. In the E-OBS map, average precipitation amounts to 684 mm/a with rainfall ranging from 273 mm/a near the Danube delta to 2218 mm/a at the Dinaric mountain peaks in the Sava basin.

The ERA5 (c) and WFDE5 (f) precipitation maps show rather smooth precipitation patterns due to the downscaling procedure without bias correction. In contrast, the ERA5-WC (d) and ERA5-GPW (e) precipitation maps feature visible topography structures due to the bias correction step included in the downscaling procedure. Here, corresponding reference climatologies used for bias correction augmented the precipitation maps with small-scale structures at a spatial resolution of 30″. ERA5 was the wettest forcing dataset with 824 mm/a precipitation on average over the whole basin. Minimum and maximum rainfall ranged from 449 mm/a in the Moldovan Plain to 1943 mm/a in the eastern Alps. In the Alps and the Alpine foreland, rainfall patterns in the ERA5 map are rather evenly distributed and show little of the more complex structures that are visible in the SAS and E-OBS maps of observed precipitation (especially the inner-Alpine dry valleys of the Inn catchment in the south-western part of the Upper Danube). In the southern Sava basin and in the Carpathian region, patchy rainfall patterns are visible. ERA5-WC was the driest forcing dataset with 754 mm/a precipitation on average with rainfall ranging from 337 mm/a near the Danube delta to 2516 mm/a around the Alpine and Dinaric mountain peaks in the Drava and Sava basins. The ERA5-WC precipitation patterns in the Alpine region (especially the inner-Alpine dry valleys), in the Dinaric region and in the Lower Danube around the southern Carpathian region are strikingly similar to the structures in the E-OBS rainfall map. In the ERA5-GPW forcing dataset, average precipitation amounted to 764 mm/a with rainfall ranging from 337 mm/a in the Danube delta (like ERA5-WC) to very high local maxima of 3225 mm/a at single mountain peaks in the northern Sava basin. In the ERA5-GPW precipitation map, a strong resemblance to the SAS map is noticeable for the Alpine region: first, the distinct rainfall band in the Alpine foreland extending far to the east, second, the pronounced inner-Alpine dry valleys of the Inn catchment in the south-western Upper Danube and third, the round-shaped dry region at the transition between the Alps and the

Dinarides in the Drava basin. The WFDE5 forcing dataset yielded an average precipitation of 788 mm/a with rainfall ranging from 278 mm/a near the Danube delta to 2251 mm/a at single mountain peaks in the northern Sava basin. The likewise smooth WFDE5 precipitation patterns in the map are quite similar to the ERA5 patterns with a few spatial shifts due to the WFD bias correction and with some more indications of Alpine precipitation patterns (e.g. the inner-Alpine dry valleys and the round-shaped dry region in the Drava basin) that are visible in the SAS and E-OBS observation maps.

3.2. Temperature, precipitation, evapotranspiration and percent bias of discharge

The percent bias (PBIAS) of discharge is an important quality criterion in hydrological modelling, as it provides information on whether the water volume of the modelled discharge in a basin is well predicted or rather over- or underestimated. In Table 3 and Fig. 5, we show the modelled long-term annual means of temperature [°C], precipitation [mm/a] and evapotranspiration [mm/a] as well as PBIAS of discharge [%] for the period 1980–2016 in the DRB and its sub basins for the simulation runs driven by ERA5, ERA5-WC, ERA5-GPW and WFDE5. Here, long-term annual mean temperature, precipitation and evapotranspiration are given as area-averaged values, which were calculated for the whole basin area upstream of the basin's associated gauge station (see Table 2). Apparently, there was much more variation in precipitation and PBIAS than in temperature and evapotranspiration between the different forcing datasets and consequently, simulation runs. The downscaled uncorrected ERA5 forcing dataset gave highest precipitation in most of the sub basins, i.e. the Upper and Middle Danube (gauges Achleiten, Bezdan), the Mures, Tisza and Siret tributary basins and the Danube overall (outlet gauge Ceatal Izmail) compared to the other forcing datasets. In most of these sub basins, also evapotranspiration – and in a lesser extent temperature – showed highest values for ERA5. Higher annual precipitation in most Danube sub basins and the Danube overall coincided with more or less high positive PBIAS (esp. the Mures and Tisza basins) for ERA5. In contrast, the Sava basin showed least precipitation for the ERA5 forcing dataset, which coincided with a relatively high negative PBIAS. Introducing bias correction of ERA5 with the global WorldClim 2 climatologies (ERA5-WC forcing dataset) led to a significant reduction of precipitation in the Upper and Middle Danube (gauges Achleiten, Bezdan), the Mures, Tisza and Siret tributary basins and the Danube overall on the one hand, and to an increase of precipitation in the Drava and Sava basins on the other. At the same time, PBIAS turned negative in the Upper Danube and more positive in the Drava basin. For the ERA5-WC forcing dataset, the more or less highly positive PBIAS in the Mures, Tisza and Siret basins and the Danube overall resulting from ERA5 were mitigated due to the reduction of precipitation. In total, PBIAS was especially low in the Danube overall at gauge Ceatal Izmail. Similarly, the negative PBIAS in the Sava basin resulting from ERA5 was slightly mitigated in ERA5-WC. The additional integration of the regional precipitation climatologies GLOWA and PRISM for the Alpine and Dinaric region into the bias correction process of ERA5 (ERA5-GPW forcing dataset) led to an increase of precipitation in the Upper and Middle Danube (gauges Achleiten, Bezdan) and also slightly in the Sava basin. At the same time, precipitation in the Drava basin decreased to about the same magnitude as in the uncorrected ERA5 forcing dataset. For the ERA5-GPW forcing dataset, the negative PBIAS in the Upper Danube and the positive PBIAS in the Drava basin resulting from the ERA5-WC forcing dataset was mitigated. Moreover, the negative PBIAS in the Sava basin resulting from ERA5 and ERA5-WC was slightly mitigated for ERA5-GPW. For the WFDE5 forcing dataset, precipitation increased again in the Upper and Middle Danube (gauge Bezdan), the Mures, Tisza and Siret tributary basins and the Danube overall, which coincided with more positive PBIAS

Table 3
Long-term annual means of temperature [°C], precipitation [mm/a], evapotranspiration [mm/a] and PBIAS of discharge [%] in the Danube and its sub basins for the period 1980–2016 as modelled by the forcing datasets ERA5, ERA5-WC, ERA5-GPW and WFDE5.

	Temperature [°C]				Precipitation [mm/a]			
Sub basin	ERA5	ERA5-WC	ERA5-GPW	WFDE5	ERA5	ERA5-WC	ERA5-GPW	WFDE5
Upper Danube	7.0	7.1	7.1	7.4	1143	994	1095	1054
Upper + Middle Danube	8.4	8.3	8.3	8.6	912	825	873	882
Drava	7.7	7.7	7.7	7.8	1017	1119	1035	1003
Sava	10.2	9.8	9.8	10.0	984	1061	1083	1040
Mures	8.4	8.0	8.0	8.1	863	656	656	693
Tisza	9.3	9.0	9.0	9.1	805	682	682	721
Siret	7.9	8.1	8.1	7.9	758	582	582	690
Danube overall	9.4	9.2	9.2	9.4	830	761	772	795
	Evapotranspiration [mm/a]				PBIAS of discharge [%]			
Sub basin	ERA5	ERA5-WC	ERA5-GPW	WFDE5	ERA5	ERA5-WC	ERA5-GPW	WFDE5
Upper Danube	521	524	527	511	+8.4	−17.5	−1.1	−5.8
Upper + Middle Danube	515	510	512	500	+22.1	−1.9	+11.3	+18.4
Drava	530	539	543	519	+16.0	+36.5	+15.6	+12.8
Sava	566	571	572	540	−29.6	−17.8	−14.6	−16.4
Mures	535	506	506	492	+72.1	−16.2	−16.2	+38.5
Tisza	521	504	504	495	+80.8	+24.3	+24.3	+46.1
Siret	492	469	469	470	+56.9	−26.4	−26.4	+24.2
Danube overall	519	510	511	497	+26.8	+4.7	+8.5	+20.0

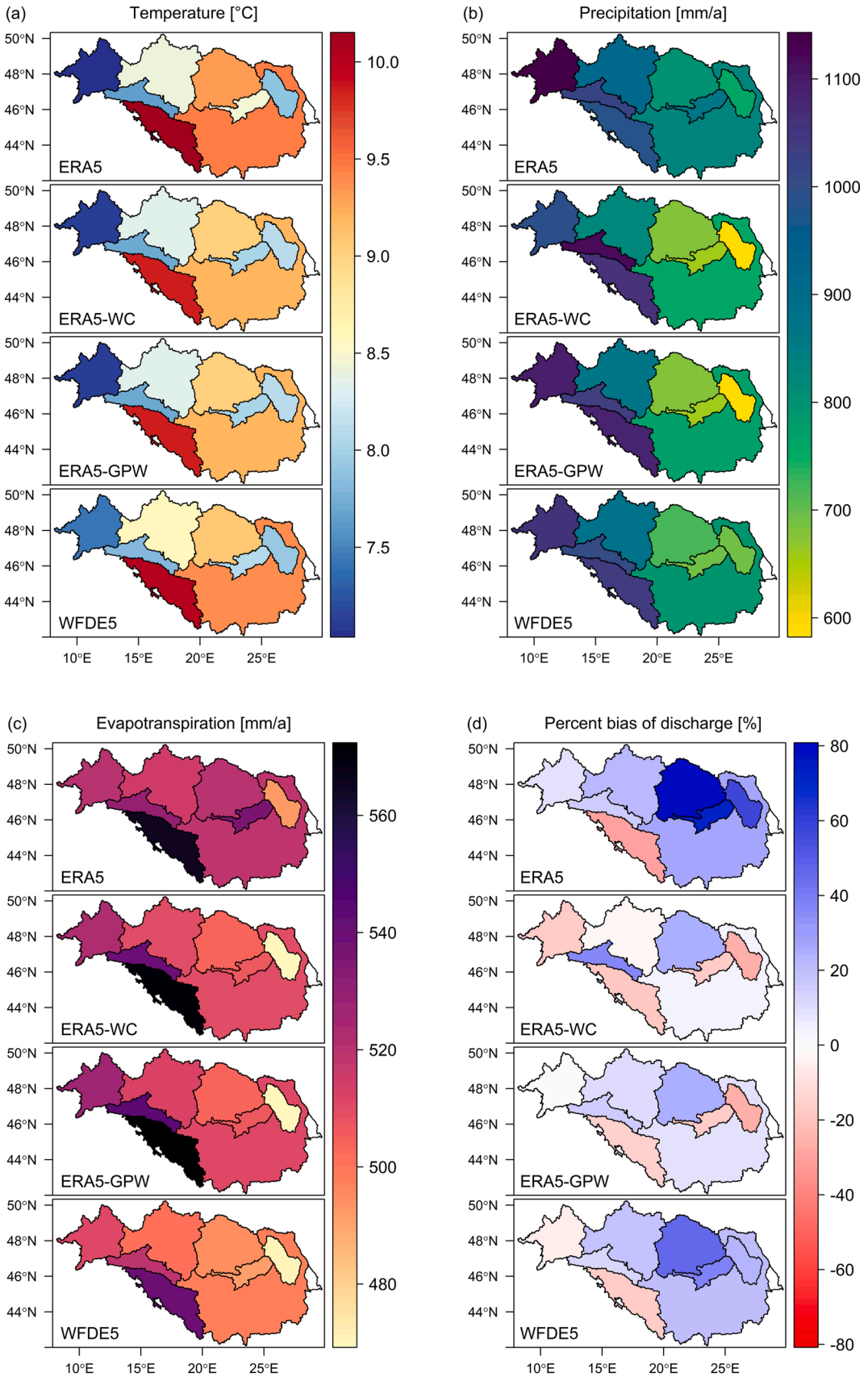

(caption on next page)

Fig. 5. Long-term annual means of temperature [°C] (a), precipitation [mm/a] (b), evapotranspiration [mm/a] (c) and PBIAS of discharge [%] (d) in the Danube and its sub basins for the period 1980–2016 as modelled by the forcing datasets ERA5, ERA5-WC, ERA5-GPW and WFDE5.

values in those basins. Compared to the other forcing datasets, WFDE5 showed intermediate precipitation values for most sub basins and highest temperature values for the Upper and Middle Danube (gauges Achleiten, Bezdan) and the Drava basin. Interestingly, the WFDE5 forcing dataset gave smallest PBIAS for the Drava (+12.8%) and Siret basins (+24.2%) compared to the other forcing datasets. However, for the majority of the sub basins, smallest PBIAS values were obtained with the ERA5-WC and ERA5-GPW forcing datasets. ERA5-GPW yielded smallest PBIAS for the Upper Danube at gauge Achleiten (−1.1%) and for the Sava basin (−14.6%). ERA5-WC yielded smallest PBIAS for the Upper and Middle Danube at gauge Bezdan (−1.9%) and for the Danube overall at gauge Ceatal Izmail (+4.7%). For two tributary basins of the Lower Danube, smallest PBIAS were equally obtained by ERA5-WC and ERA5-GPW, i.e. the Mures basin (−16.2%) and the Tisza basin (+24.3%). ERA5 did not show smallest PBIAS values in any of the sub basins.

3.3. Model efficiency based on daily discharge

In Table 4 and Fig. 6, we show model efficiencies (NSE and KGE) based on observed and modelled daily discharge as modelled by the ERA5, ERA5-WC, ERA5-GPW and WFDE5 forcing datasets for the period 1980–2016 for the Danube and its sub basins. In comparison to all other simulation runs, the ERA5-driven simulation showed poorest results for the majority of sub basins (esp. the tributary basins of the Lower Danube) concerning NSE and KGE. Especially low model efficiencies were achieved in the Mures and Tisza basins (NSE < 0) for ERA5. In contrast, relatively high model efficiencies were achieved for the Upper Danube (gauge Achleiten) and the Drava basin. The poor ERA5 model efficiencies especially in the Sava, Mures, Tisza and Siret basins and the Danube overall (gauge Ceatal Izmail) could be significantly improved by ERA5-WC. However, model efficiencies of the ERA5-WC-driven simulation slightly declined in the Upper Danube (gauge Achleiten) and vastly dropped in the Drava basin to NSE < 0 in comparison to ERA5. Through the additional introduction of the regional precipitation climatologies GLOWA and PRISM for the bias correction in the Alps and Dinarides, the ERA5-GPW-driven simulation showed improved model efficiencies especially for the Upper Danube, the Drava and the Sava basins. In comparison to ERA5-GPW, discharges from the WFDE5-driven simulation showed lower efficiencies for the majority of sub basins with especially low results for the Mures and Tisza basins. In contrast, the WFDE5-driven simulation showed best model efficiencies for the Drava (NSE = 0.66, KGE = 0.83), the Sava (NSE = 0.66, KGE = 0.66) and the Siret basin (NSE = 0.54, KGE = 0.57) in comparison to all other forcing datasets. For the Upper Danube (gauge Achleiten), best NSE was obtained with the ERA5-GPW-driven simulation (NSE = 0.75), whereas best KGE was obtained with the ERA5-driven simulation (KGE = 0.83; although KGE was very similar for ERA5, ERA5-GPW and WFDE5). For two tributary basins of the Lower Danube, efficiency measures were equally best for ERA5-WC and ERA5-GPW (NSE = 0.47 and KGE = 0.69 for the Mures and NSE = 0.39 and KGE = 0.54 for the Tisza basin). Moreover, ERA5-WC yielded best efficiencies for the Upper and Middle Danube at gauge Bezdan (NSE = 0.71, KGE = 0.78) and for the Danube overall at gauge Ceatal Izmail (NSE = 0.70, KGE = 0.77). Also for these two basins, KGE values were very similar for the ERA5-WC-driven and the ERA5-GPW-driven simulation.

4. Discussion

4.1. Performance of the uncalibrated hydrological model

Our results showed that satisfactory model results in terms of the goodness-of-fit criteria PBIAS, NSE and KGE could be equally achievable without extensive model calibration. Considering the fact that no calibration with observed discharge has been undertaken at all, we obtained satisfactory results by using a reasonably and comprehensively parameterized mechanistic hydrological model, which takes physical processes of water flows into account due to its process-based nature. Also for methodological reasons, it is appropriate to dispense with calibration so that the hydrological model is not parameterized differently for each meteorological forcing dataset. Calibration that aims to best fit the discharge observations would prevent an objective comparison of the suitability of the different meteorological drivers for hydrological modelling applications from the outset.

The NSE results obtained in our study are in good accordance compared to other model studies, where extensive calibration efforts have been undertaken. In Table 5, we show NSE of daily discharges from the respective best simulation run in this study compared to the daily NSE of validation obtained at the exact or nearby gauges from the study of Stagl and Hattermann (2015). As can be seen, our NSE were quite similar to the NSE given in the comparative study and were even better for the Upper Danube, the Upper and Middle Danube (NSE at Bezdan/Bratislava gauges), the Drava and the Siret basin.

Concerning the relationship between NSE and KGE across all sub basins and all simulation runs, our results gave a positive linear correlation between NSE and KGE values. This means that higher NSE tended to be associated with higher KGE and vice versa (see Fig. 7). KGE is often used in addition to or instead of NSE to account for specific shortcomings of NSE. With KGE, it is possible to rate the model's ability to yield simultaneously good solutions for the linear correlation, the bias and the variability of flow, which is not the case with NSE (Gupta et al., 2009). As Knoben et al. (2019) vividly showed, an exemplary strength of KGE is the ability to capture a model's potential tendency to overestimate discharge peaks (which NSE cannot) and in contrast, an exemplary strength of NSE is the ability to capture potential systematic offsets between the modelled and the observed hydrograph (which KGE cannot). A positive correlation of NSE and KGE therefore indicates that there are no one-sided deficiencies in the physically-based description of hydrological processes in PROMET that would manifest as systematic over- or underestimations of the modelled hydrograph or a

systematic overestimation of modelled flood peaks.

4.2. Performance of the meteorological forcing datasets and climatologies for bias correction

Our results showed that sub basin-specific variations in long-term annual means of precipitation between the different forcing datasets and thus, simulation runs were much greater than of temperature or evapotranspiration, connected with corresponding impacts on PBIAS. Sub basin-specific higher PBIAS values (positive or negative) coincided primarily with variations in forcing data-specific precipitation between the different simulation runs and very little with variations in temperature or evapotranspiration. This clearly suggests that a small PBIAS and thus, well predicted water budget within a basin is above all dependent on the correct representation of precipitation in the meteorological data and underlines the importance of choosing appropriate precipitation forcing data as input for hydrological modelling, combined with suitable climatologies especially for precipitation bias correction.

The uncorrected ERA5 forcing dataset showed highest annual mean precipitation for most sub basins (except for Drava and Sava), leading to systematic positive PBIAS for the ERA5-driven simulation in these sub basins. The poor performance of the ERA5-driven simulation concerning NSE and KGE compared to the other simulations may be traced back to the relatively smooth patterns in the downscaled ERA5 precipitation map, especially over mountainous terrain (see Fig. 4). In mountain regions, the ERA5 precipitation map sharply contrasted with the SAS and E-OBS maps of observed precipitation, both of which showed detailed small-scale rainfall structures in the Alps, the Dinarides and the Carpathians, especially inner-Alpine dry valleys and drier regions in the Drava basin. This suggests that the smooth precipitation patterns in ERA5 may have led to a distortion of spatial runoff dynamics and to an inadequate emulation of the hydrograph. Interestingly, the downscaled WFDE5 forcing dataset showed similar smooth precipitation patterns compared to the downscaled uncorrected ERA5 reanalysis, but the WFDE5-driven simulation yielded much better results in terms of PBIAS, NSE and KGE in almost all sub basins compared to the ERA5-driven simulation. WFDE5 even yielded best NSE and KGE for the mountain watersheds Drava and Sava and also for the Siret basin across all forcing datasets. Apparently, the WFD bias correction methodology used to create WFDE5 offers great benefits for hydrological modelling purposes in the DRB.

Another aspect, which is particularly important in mountainous regions, may also be a determining factor for the good performance of WFDE5 in the mountain watersheds: the presence of undercatch correction. Especially in mountainous regions, a major source of uncertainty is systematic measurement bias due to wind-induced undercatch at precipitation gauging stations. This is particularly significant in wind-exposed areas and during snowfall periods, leading to systematic underestimations of precipitation (Sevruk, 2005). In contrast to all other forcing datasets, precipitation climatologies and observation datasets presented in this study (ERA5, WorldClim 2, PRISM, GLOWA and E-OBS), the WFDE5 forcing dataset is in fact the only one, which includes an undercatch correction (Cornes et al., 2018; Cucchi et al., 2020; Fick and Hijmans, 2017; Frei and Schär, 1998; Früh et al., 2006). Although the mountainous Upper Danube, Drava and Sava basins featured highest area-averaged precipitation means in the ERA5, ERA5-WC and ERA5-GPW forcing datasets and not in the WFDE5 dataset, absent undercatch correction can nevertheless lead to local underestimations of rainfall at higher altitudes within the sub basins. This may result in inadequately predicted dynamics of discharge formation and to a possible distortion of the hydrograph. Therefore, a possible explanation for the best model efficiencies of WFDE5 in the Drava, the Sava and the Siret basins may well be the presence of both bias correction and undercatch correction in the WFDE5 dataset, leading to better predicted dynamics of the mountain watershed hydrology.

Concerning ERA5, the introduction of bias correction vastly reduced PBIAS and improved NSE and KGE for the simulations driven by ERA5-WC and ERA5-GPW compared to the simulation driven by the uncorrected ERA5 reanalysis. Solely incorporating the global WorldClim 2 temperature and precipitation climatologies for bias correction (ERA5-WC) led to smaller PBIAS values and improved model efficiency especially in the Lower Danube and its tributary basins, where WorldClim 2 significantly reduced precipitation amounts. In contrast, in the complex terrains of the Alps and Dinarides (esp. Upper Danube and Drava basin), WorldClim 2 indeed added some structure to the precipitation map, but did not appear to reproduce the complex actual precipitation patterns in an eligible way as NSE and KGE considerably dropped compared to the ERA5-driven simulation. This is particularly interesting given that the spatial patterns in the ERA5-WC precipitation map in the Alps and Dinarides (Fig. 4) were in close correspondence to the patterns in the E-OBS precipitation map, but not to those in the SAS map. This similarity may well be due to the fact that WorldClim 2 and E-OBS incorporate overlapping precipitation stations across Europe. E-OBS is created from data by the European Climate Assessment and

Table 4
Nash-Sutcliffe efficiency (NSE) and Kling-Gupta efficiency (KGE) of modelled and observed daily discharge in the Danube and its sub basins for the period 1980–2016 as modelled by the forcing datasets ERA5, ERA5-WC, ERA5-GPW and WFDE5.

	NSE				KGE			
Sub basin	ERA5	ERA5-WC	ERA5-GPW	WFDE5	ERA5	ERA5-WC	ERA5-GPW	WFDE5
Upper Danube	0.66	0.53	0.75	0.71	0.83	0.73	0.81	0.80
Upper + Middle Danube	0.41	0.71	0.66	0.57	0.71	0.78	0.75	0.73
Drava	0.51	−0.09	0.51	0.66	0.79	0.60	0.78	0.83
Sava	0.39	0.60	0.63	0.66	0.57	0.62	0.62	0.66
Mures	−1.23	0.47	0.47	0.06	0.24	0.69	0.69	0.55
Tisza	−0.98	0.39	0.39	0.15	0.12	0.54	0.54	0.46
Siret	0.26	0.46	0.46	0.54	0.30	0.55	0.55	0.57
Danube overall	0.12	0.70	0.66	0.56	0.68	0.77	0.75	0.75

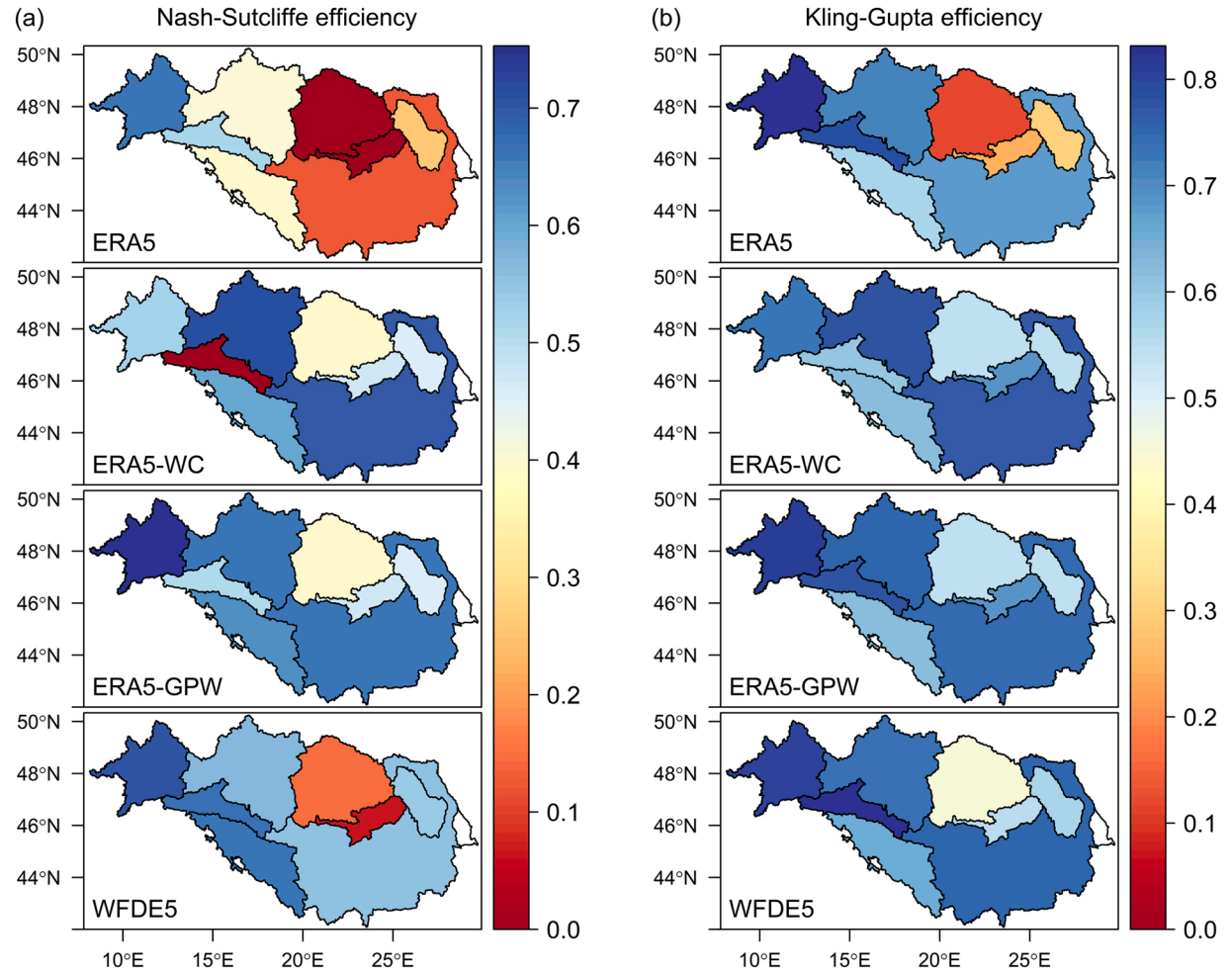

Fig. 6. Nash-Sutcliffe efficiency (a) and Kling-Gupta efficiency (b) of modelled and observed daily discharge in the Danube and its sub basins for the period 1980–2016 as modelled by the forcing datasets ERA5, ERA5-WC, ERA5-GPW and WFDE5 (Note: for clearer visualization, negative NSE are displayed as 0).

Table 5
Comparison of Nash-Sutcliffe efficiencies (NSE) of daily discharges in this study to daily NSE of validation from Stagl and Hattermann (2015) in the Danube and its sub basins.

	This study			Study of Stagl and Hattermann (2015)	
Sub basin	Gauge	Forcing dataset yielding best NSE	NSE	Gauge	NSE
Upper Danube	Achleiten	ERA5-GPW	0.75	Achleiten	0.69
Upper + Middle Danube	Bezdan	ERA5-WC	0.71	Bratislava / Bazias	0.62 / 0.74
Drava	Dravaszabolcs	WFDE5	0.66	Borl	0.41
Sava	Sremska Mitrovica	WFDE5	0.66	Sremska Mitrovica	0.77
Mures	Nagylak	ERA5-WC/ERA5-GPW	0.47	Arad	0.67
Tisza	Senta	ERA5-WC/ERA5-GPW	0.39	Szeged	0.54
Siret	Lungoci	WFDE5	0.54	Lungoci	0.51
Danube overall	Ceatal Izmail	ERA5-WC	0.70	Ceatal Izmail	0.76

Dataset (ECA&D) initiative (Klein Tank et al., 2002; Klok and Klein Tank, 2009), sourcing station data from many National Meteorological Services (NMS) and other providers across Europe (Cornes et al., 2018). The WorldClim 2 station data basis is mainly compiled from global datasets like CRU TS3.22 station observations, some of which are shared by numerous national weather services through the World Meteorological Organization (WMO) (Harris et al., 2014). However, a considerable proportion of the station data basis for WorldClim 2 also directly originates from the ECA&D pool. In addition to the directly included ECA&D stations, there is also a larger number of stations in Europe which are duplicated in ECA&D and global sources used for WorldClim 2 (Fick and Hijmans, 2017).

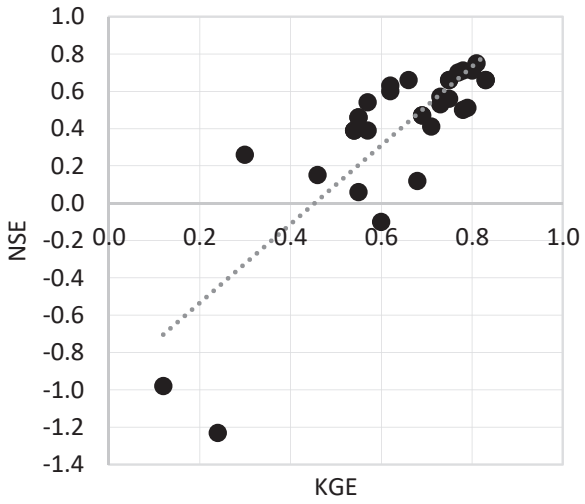

Fig. 7. Relationship between Nash-Sutcliffe efficiency (NSE) and Kling-Gupta efficiency (KGE) for all sub basins and all simulation runs in the Danube River Basin.

As Fick and Hijmans (2017) and Hijmans et al. (2005) stated, there are greater uncertainties in the WorldClim 2 precipitation climatology in mountainous terrain, mainly due to the lower station density and the simplifying assumption of an elevation dependence of precipitation in the spatial interpolation routine. Uncertainties were also reported for the E-OBS precipitation dataset in mountainous and data-scarce regions (Cornes et al., 2018). In contrast, Frei and Schär (1998) argued that precipitation-elevation correlations should only be used very carefully when interpolating station data in the Alpine region. They pointed out that precipitation measured at stations is highly dependent on broader-scale synoptic characteristics and topographical factors like slope or exposure (summit vs. valley location, windward vs. leeward aspect), which lead to particular variations in the Alpine region and especially across the Alpine ridge (Frei and Schär, 1998). The relatively high uncertainties for precipitation in mountainous terrain in WorldClim 2 could be the reason for overestimations of precipitation at highest elevations in the Danube basin and excess precipitation especially in the Drava basin connected with a highly positive PBIAS. Excess rainfall at highest elevations in the model may also have caused an inadequate simulation of runoff volume, dynamics and timing and may have resulted in a hydrograph yielding poor NSE and KGE in the Drava and Upper Danube basins.

We learned that the additional integration of the regional precipitation climatologies GLOWA and PRISM in the bias correction routine of precipitation (ERA5-GPW) led to better results concerning PBIAS, NSE and KGE in the Upper Danube, Drava and Sava basins than the bias correction with the WorldClim 2 precipitation climatology alone (ERA5-WC). An interesting finding here is that the ERA5-GPW precipitation map (Fig. 4) showed very similar spatial patterns in the Alps and Dinarides compared to the SAS map (in particular, the distinct rainfall band in the Bavarian Alpine foreland, the inner-Alpine dry valleys of the Inn catchment in the southwestern Upper Danube and the round-shaped dry region in the Drava basin). In contrast, the ERA5-GPW map did not resemble the E-OBS map in these regions. In total, the described precipitation patterns resulted in a higher basin precipitation in the Upper Danube for ERA5-GPW and in a much smaller PBIAS compared to ERA5-WC. Thus, the reduced PBIAS and the improved model efficiencies for the Upper Danube, Drava and Sava basins may indicate that the ERA5-GPW precipitation map (which was similar to the SAS map) showed more realistic spatial precipitation patterns in the Alpine region than the ERA5-WC map (which was similar to the E-OBS map). We assume that the underlying higher station density for the generation of the regional precipitation climatologies GLOWA and PRISM leads to a much more realistic reproduction of the actual spatial precipitation patterns in the Alps and Dinarides than WorldClim 2 is able to provide. This is a strong indication that observation datasets should not be considered trustworthy based on their mere observational nature. Taking observational uncertainties into account, the selection of an appropriate reference climatology dataset for bias correction should be handled just as critically as, for example, the selection of an appropriate bias correction method.

5. Summary and conclusions

In this paper, we analysed the performance of the global meteorological reanalysis ERA5 and the global bias-adjusted forcing dataset WFDE5 for driving the physically-based hydro-agroecological model PROMET in the large, heterogeneous Danube River Basin. Furthermore, we investigated the suitability of the global to regional reference climatologies WorldClim 2, GLOWA and PRISM for linear bias correction of ERA5 temperature and precipitation incorporated in the downscaling routine. We performed four uncalibrated hydrological simulation runs of 30″ spatial and hourly temporal resolution for the period 1980–2016 driven by the following configurations of meteorological forcing data:

- the uncorrected ERA5 reanalysis (denoted as ERA5),
- the WFDE5 forcing dataset bias-corrected according to the WFD methodology (denoted as WFDE5),

- the ERA5 reanalysis bias-corrected with the WorldClim 2 temperature and precipitation climatologies (denoted as ERA5-WC),
- the ERA5 reanalysis bias-corrected with the WorldClim 2 temperature climatology and a mosaic of the GLOWA and PRISM Alpine precipitation climatologies and the WorldClim 2 precipitation climatology (denoted as ERA5-GPW).

Our simulations showed significant differences in performance between the different meteorological forcing datasets ERA5, WFDE5, ERA5-WC and ERA5-GPW. We evaluated the performance of the simulation runs using the PBIAS of discharge and the model efficiency metrics NSE and KGE, calculated from modelled and observed daily discharge at selected gauges in the Danube basin and its sub basins. The ERA5-GPW-driven simulation yielded the smallest PBIAS values and the best model efficiencies across the majority of sub basins compared to the other simulation runs. Given the poor performance of the ERA5-driven simulation in terms of PBIAS, NSE and KGE across nearly all sub basins, bias correction is essential for hydrological modelling in the DRB. Compared to ERA5, the WFDE5-driven simulation yielded much better results in terms of PBIAS, NSE and KGE (with even best NSE and KGE in the mountainous Drava and Sava basins). This could be due to the WFD bias correction and the undercatch correction applied in WFDE5, which is apparently very suitable for hydrological modelling purposes. Concerning ERA5, we learned that bias correction with the global and widely used WorldClim 2 temperature and precipitation climatology alone (ERA5-WC forcing dataset) significantly improved the Lower Danube and its tributary basins in terms of PBIAS, NSE and KGE. However, WorldClim 2 was insufficient to capture the complex spatial precipitation patterns in mountainous terrain in the Alps and Dinarides, which are located in the Upper Danube, Drava and Sava basins. Here, the greater uncertainties in the interpolation of precipitation in mountainous terrain are likely to be a major limitation. Instead, additionally incorporating the regional high-resolution GLOWA and PRISM Alpine precipitation climatologies (derived from a much higher underlying station density in the European Alps) in the bias correction routine of ERA5 (ERA5-GPW forcing dataset) noticeably added distinct small-scale spatial precipitation patterns in the Alps and Dinarides. This approach reduced PBIAS values and improved model efficiencies for the mountain watersheds Upper Danube, Drava and Sava in comparison to the bias correction with WorldClim 2 alone.

We draw three major conclusions from the findings of our simulation study:

First, we have shown that with a reasonable and comprehensive parametrization of a process-based hydrological model such as PROMET, satisfying results for PBIAS, NSE and KGE can be obtained without extensive calibration of model parameters to best fit measured discharges. The ability of PROMET to simulate water flows, runoff formation and flood propagation in the channel through a physical process description without "trial-and-error" calibration was the prerequisite to perform an objective comparison of different meteorological forcing datasets in the next step.

Second, we have demonstrated the applicability of the global meteorological reanalysis ERA5 (with appropriate bias correction as a prerequisite) and the global bias-adjusted forcing dataset WFDE5 for hydrological modelling. We obtained satisfying results for PBIAS, NSE and KGE at a comparatively fine spatial resolution of 30″ even in a hydrologically complex, large and diverse basin such as the Danube. Nevertheless, we have shown that appropriate bias correction, especially of precipitation, is an essential part of the downscaling routine of the ERA5 reanalysis for driving hydrological models in the DRB.

Third, we emphasize the need for regional high-resolution precipitation climatologies for the precipitation bias correction process of reanalyses for hydrological modelling applications in topographically complex mountain terrains such as the Alps and Dinarides. High-resolution precipitation climatologies such as GLOWA and PRISM, created from high station density, can more adequately account for small-scale precipitation patterns. In contrast, global climatologies created from lower station density quickly reach their limits. Based on our findings, we therefore argue that the choice of an appropriate reference climatology dataset for bias correction of precipitation in Alpine terrain is of utmost importance and needs to be carefully considered.

Further research must be undertaken to determine whether and to what extent the need for regional high-resolution precipitation climatologies for bias correction applies for other mountainous regions around the globe. It seems plausible that this issue is not unique to the European Alps. In this light, our results also emphasize the importance of further research to develop appropriate reanalysis schemes for mountainous regions of much higher spatial resolution with the ultimate goal of eventually eliminating the need for downscaling and bias correction of meteorological forcing data for hydrological modelling.

CRediT authorship contribution statement

Elisabeth Probst: Conceptualization, Methodology, Software, Validation, Formal analysis, Investigation, Data curation, Writing – original draft preparation, Writing – review & editing, Visualization. **Wolfram Mauser:** Conceptualization, Methodology, Software, Resources, Writing – review & editing, Supervision, Project administration, Funding acquisition.

Declaration of Competing Interest

The authors declare that they have no known competing financial interests or personal relationships that could have appeared to influence the work reported in this paper.

Acknowledgements

This work was supported by the German Federal Ministry of Education and Research (BMBF) within its funding measure "Water as a Global Resource" (GRoW) [grant number 02WGR1423A], which is part of the "Research for Sustainable Development (FONA)" framework. We thank the editor and an anonymous reviewer for critically reading an earlier draft of the manuscript and providing

helpful comments and suggestions to improve and clarify the manuscript.

Appendix A. Supporting information

Supplementary data associated with this article can be found in the online version at doi:10.1016/j.ejrh.2022.101023.

References

Abbaspour, K.C., Rouholahnejad, E., Vaghefi, S., Srinivasan, R., Yang, H., Kløve, B., 2015. A continental-scale hydrology and water quality model for Europe: Calibration and uncertainty of a high-resolution large-scale SWAT model. J. Hydrol. 524, 733–752. https://doi.org/10.1016/j.jhydrol.2015.03.027.

Beck, H.E., Vergopolan, N., Pan, M., Levizzani, V., van Dijk, A.I.J.M., Weedon, G.P., Brocca, L., Pappenberger, F., Huffman, G.J., Wood, E.F., 2017. Global-scale evaluation of 22 precipitation datasets using gauge observations and hydrological modeling. Hydrol. Earth Syst. Sci. 21 (12), 6201–6217. https://doi.org/10.5194/hess-21-6201-2017.

Brooks, R.H., Corey, A.T., 1964. Hydraulic properties of porous media. Hydrol. Pap., 3. Colo. State Univ. Fort Collins 27.

Chen, D.-X., Coughenour, M.B., Knapp, A.K., Owensby, C.E., 1994. Mathematical simulation of C_4 grass photosynthesis in ambient and elevated CO_2. Ecol. Modell. 73 (1), 63–80. https://doi.org/10.1016/0304-3800(94)90098-1.

Chen, J., Brissette, F.P., Chaumont, D., Braun, M., 2013. Finding appropriate bias correction methods in downscaling precipitation for hydrologic impact studies over North America. Water Resour. Res. 49 (7), 4187–4205. https://doi.org/10.1002/wrcr.20331.

Chen, J., Brissette, F.P., Chen, H., 2018. Using reanalysis-driven regional climate model outputs for hydrology modelling. Hydrol. Process. 32 (19), 3019–3031. https://doi.org/10.1002/hyp.13251.

Cornes, R.C., van der Schrier, G., van den Besselaar, E.J.M., Jones, P.D., 2018. An ensemble version of the E-OBS temperature and precipitation data sets. J. Geophys. Res. Atmos. 123 (17), 9391–9409. https://doi.org/10.1029/2017JD028200.

Cucchi, M., Weedon, G.P., Amici, A., Bellouin, N., Lange, S., Müller Schmied, H., Hersbach, H., Buontempo, C., 2020. WFDE5: bias-adjusted ERA5 reanalysis data for impact studies. Earth Syst. Sci. Data 12 (3), 2097–2120. https://doi.org/10.5194/essd-12-2097-2020.

Cunge, J.A., 1969. On the subject of a flood propagation computation method (Muskingum Method). J. Hydraul. Res. 7 (2), 205–230. https://doi.org/10.1080/00221686909500264.

Dee, D.P., Uppala, S.M., Simmons, A.J., Berrisford, P., Poli, P., Kobayashi, S., Andrae, U., Balmaseda, M.A., Balsamo, G., Bauer, P., Bechtold, P., Beljaars, A.C.M., van de Berg, L., Bidlot, J., Bormann, N., Delsol, C., Dragani, R., Fuentes, M., Geer, A.J., Haimberger, L., Healy, S.B., Hersbach, H., Hólm, E.V., Isaksen, L., Kållberg, P., Köhler, M., Matricardi, M., McNally, A.P., Monge-Sanz, B.M., Morcrette, J.J., Park, B.K., Peubey, C., de Rosnay, P., Tavolato, C., Thépaut, J.N., Vitart, F., 2011. The ERA-Interim reanalysis: configuration and performance of the data assimilation system. Q. J. R. Meteorol. Soc. 137 (656), 553–597. https://doi.org/10.1002/qj.828.

Döll, P., Fiedler, K., Zhang, J., 2009. Global-scale analysis of river flow alterations due to water withdrawals and reservoirs. Hydrol. Earth Syst. Sci. 13 (12), 2413–2432. https://doi.org/10.5194/hess-13-2413-2009.

Essou, G.R.C., Brissette, F., Lucas-Picher, P., 2017. The use of reanalyses and gridded observations as weather input data for a hydrological model: comparison of performances of simulated river flows based on the density of weather stations. J. Hydrometeorol. 18 (2), 497–513. https://doi.org/10.1175/JHM-D-16-0088.1.

Essou, G.R.C., Sabarly, F., Lucas-Picher, P., Brissette, F., Poulin, A., 2016. Can precipitation and temperature from meteorological reanalyses be used for hydrological modeling? J. Hydrometeorol. 17 (7), 1929–1950. https://doi.org/10.1175/JHM-D-15-0138.1.

European Environmental Agency (EEA), 2012. CORINE Land Cover (CLC2012). ⟨https://land.copernicus.eu/pan-european/corine-land-cover/clc-2012⟩. (Accessed 30 July 2021).

European Space Agency (ESA), 2015. Land Cover CCI Product User Guide Version 2 Tech. Rep. ⟨http://maps.elie.ucl.ac.be/CCI/viewer/download/ESACCI-LC-Ph2-PUGv2_2.0.pdf⟩. (Accessed 30 July 2021).

EUROSTAT, 2013. Crops by classes of utilised agricultural area in number of farms and hectare by NUTS 2 regions (ef_lus_allcrops). ⟨https://ec.europa.eu/eurostat/web/agriculture/data/database⟩. (Accessed 30 July 2021).

EUROSTAT, 2021. Crop production in EU standard humidity (from 2000 onwards) (apro_cpsh). ⟨https://ec.europa.eu/eurostat/web/agriculture/data/database⟩. (Accessed 30 July 2021).

FAO/IIASA/ISRIC/ISSCAS/JRC, 2012. Harmonized World Soil Database (version 1.2). Rome, Italy and Laxenburg, Austria. ⟨http://www.fao.org/soils-portal/soil-survey/soil-maps-and-databases/harmonized-world-soil-database-v12/en/⟩. (Accessed 30 July 2021).

Farquhar, G.D., von Caemmerer, S., Berry, J.A., 1980. A biochemical model of photosynthetic CO_2 assimilation in leaves of C_3 species. Planta 149 (1), 78–90. https://doi.org/10.1007/bf00386231.

Farr, T.G., Rosen, P.A., Caro, E., Crippen, R., Duren, R., Hensley, S., Kobrick, M., Paller, M., Rodriguez, E., Roth, L., Seal, D., Shaffer, S., Shimada, J., Umland, J., Werner, M., Oskin, M., Burbank, D., Alsdorf, D., 2007. The shuttle radar topography mission. Rev. Geophys. 45 (2), 1–33. https://doi.org/10.1029/2005RG000183.

Fick, S.E., Hijmans, R.J., 2017. WorldClim 2: new 1-km spatial resolution climate surfaces for global land areas. Int. J. Climatol. 37 (12), 4302–4315. https://doi.org/10.1002/joc.5086.

Frei, C., Schär, C., 1998. A precipitation climatology of the Alps from high-resolution rain-gauge observations. Int. J. Climatol. 18 (8), 873–900. https://doi.org/10.1002/(SICI)1097-0088(19980630)18:8<873::AID-JOC255>3.0.CO;2-9.

Früh, B., Schipper, H., Pfeiffer, A., Wirth, V., 2006. A pragmatic approach for downscaling precipitation in alpine-scale complex terrain. Meteorol. Z. 15 (6), 631–646. https://doi.org/10.1127/0941-2948/2006/0137.

Gampe, D., Schmid, J., Ludwig, R., 2019. Impact of reference dataset selection on RCM evaluation, bias correction, and resulting climate change signals of precipitation. J. Hydrometeorol. 20 (9), 1813–1828. https://doi.org/10.1175/JHM-D-18-0108.1.

Global Runoff Data Centre (GRDC), 2019. The global runoff data centre. 56068 Koblenz, Germany. ⟨https://grdc.bafg.de⟩. (Accessed 30 July 2021).

Gubler, S., Hunziker, S., Begert, M., Croci-Maspoli, M., Konzelmann, T., Brönnimann, S., Schwierz, C., Oria, C., Rosas, G., 2017. The influence of station density on climate data homogenization. Int. J. Climatol. 37 (13), 4670–4683. https://doi.org/10.1002/joc.5114.

Gupta, H.V., Kling, H., Yilmaz, K.K., Martinez, G.F., 2009. Decomposition of the mean squared error and NSE performance criteria: implications for improving hydrological modelling. J. Hydrol. 377 (1), 80–91. https://doi.org/10.1016/j.jhydrol.2009.08.003.

Hank, T.B., Bach, H., Mauser, W., 2015. Using a remote sensing-supported hydro-agroecological model for field-scale simulation of heterogeneous crop growth and yield: application for wheat in Central Europe. Remote Sens. 7 (4), 3934–3965. https://doi.org/10.3390/rs70403934.

Harris, I., Jones, P.D., Osborn, T.J., Lister, D.H., 2014. Updated high-resolution grids of monthly climatic observations – the CRU TS3.10 Dataset. Int. J. Climatol. 34 (3), 623–642. https://doi.org/10.1002/joc.3711.

Hersbach, H., Bell, B., Berrisford, P., Hirahara, S., Horányi, A., Muñoz-Sabater, J., Nicolas, J., Peubey, C., Radu, R., Schepers, D., Simmons, A., Soci, C., Abdalla, S., Abellan, X., Balsamo, G., Bechtold, P., Biavati, G., Bidlot, J., Bonavita, M., Chiara, G., Dahlgren, P., Dee, D., Diamantakis, M., Dragani, R., Flemming, J., Forbes, R., Fuentes, M., Geer, A., Haimberger, L., Healy, S., Hogan, R.J., Hólm, E., Janisková, M., Keeley, S., Laloyaux, P., Lopez, P., Lupu, C., Radnoti, G., Rosnay, P., Rozum, I., Vamborg, F., Villaume, S., Thépaut, J.N., 2020. The ERA5 global reanalysis. Q. J. R. Meteorol. Soc. 146 (730), 1999–2049. https://doi.org/10.1002/qj.3803.

Hijmans, R.J., Cameron, S.E., Parra, J.L., Jones, P.G., Jarvis, A., 2005. Very high resolution interpolated climate surfaces for global land areas. Int. J. Climatol. 25 (15), 1965–1978. https://doi.org/10.1002/joc.1276.

International Commission for the Protection of the Danube River (ICPDR), 2021. Danube River Basin water quality database. Vienna, Austria. ⟨https://www.icpdr.org/wq-db/⟩. (Accessed 30 July 2021).

Jungwirth, M., Haidvogl, G., Hohensinner, S., Waidbacher, H., Zauner, G., 2014. Österreichs Donau. Landschaft – Fisch – Geschichte. Institut für Hydrobiologie u. Gewässermanagement. BOKU Wien. 420.

Kay, A.L., Rudd, A.C., Davies, H.N., Kendon, E.J., Jones, R.G., 2015. Use of very high resolution climate model data for hydrological modelling: baseline performance and future flood changes. Clim. Change 133 (2), 193–208. https://doi.org/10.1007/s10584-015-1455-6.

Klein Tank, A.M.G., Wijngaard, J.B., Können, G.P., Böhm, R., Demarée, G., Gocheva, A., Mileta, M., Pashiardis, S., Hejkrlik, L., Kern-Hansen, C., Heino, R., Bessemoulin, P., Müller-Westermeier, G., Tzanakou, M., Szalai, S., Pálsdóttir, T., Fitzgerald, D., Rubin, S., Capaldo, M., Maugeri, M., Leitass, A., Bukantis, A., Aberfeld, R., van Engelen, A.F.V., Forland, E., Mietus, M., Coelho, F., Mares, C., Razuvaev, V., Nieplova, E., Cegnar, T., Antonio López, J., Dahlström, B., Moberg, A., Kirchhofer, W., Ceylan, A., Pachaliuk, O., Alexander, L.V., Petrovic, P., 2002. Daily dataset of 20th-century surface air temperature and precipitation series for the European Climate Assessment. Int. J. Climatol. 22 (12), 1441–1453. https://doi.org/10.1002/joc.773.

Kling, H., Fuchs, M., Paulin, M., 2012. Runoff conditions in the upper Danube basin under an ensemble of climate change scenarios. J. Hydrol. 424–425, 264–277. https://doi.org/10.1016/j.jhydrol.2012.01.011.

Klok, E.J., Klein Tank, A.M.G., 2009. Updated and extended European dataset of daily climate observations. Int. J. Climatol. 29 (8), 1182–1191. https://doi.org/10.1002/joc.1779.

Knoben, W.J.M., Freer, J.E., Woods, R.A., 2019. Technical note: Inherent benchmark or not? Comparing Nash–Sutcliffe and Kling–Gupta efficiency scores. Hydrol. Earth Syst. Sci. 23 (10), 4323–4331. https://doi.org/10.5194/hess-23-4323-2019.

Kotlarski, S., Szabó, P., Herrera, S., Räty, O., Keuler, K., Soares, P.M., Cardoso, R.M., Bosshard, T., Pagé, C., Boberg, F., Gutiérrez, J.M., Isotta, F.A., Jaczewski, A., Kreienkamp, F., Liniger, M.A., Lussana, C., Pianko-Kluczyńska, K., 2019. Observational uncertainty and regional climate model evaluation: a pan-European perspective. Int. J. Climatol. 39 (9), 3730–3749. https://doi.org/10.1002/joc.5249.

Kovács, P., 2010. Characterization of the runoff regime and its stability in the Danube catchment. In: Brilly, M. (Ed.), Hydrological Processes of the Danube River Basin. Springer, Dordrecht, pp. 143–173. 10.1007/978-90-481-3423-6_5.

Lafon, T., Dadson, S., Buys, G., Prudhomme, C., 2013. Bias correction of daily precipitation simulated by a regional climate model: a comparison of methods. Int. J. Climatol. 33 (6), 1367–1381. https://doi.org/10.1002/joc.3518.

Lehner, B., Verdin, K., Jarvis, A., 2008. New global hydrography derived from spaceborne elevation data. Eos 89 (10), 93–94. https://doi.org/10.1029/2008EO100001.

Malagó, A., Bouraoui, F., Vigiak, O., Grizzetti, B., Pastori, M., 2017. Modelling water and nutrient fluxes in the Danube River Basin with SWAT. Sci. Total Environ. 603–604, 196–218. https://doi.org/10.1016/j.scitotenv.2017.05.242.

Marke, T., Mauser, W., Pfeiffer, A., Zängl, G., Jacob, D., Strasser, U., 2014. Application of a hydrometeorological model chain to investigate the effect of global boundaries and downscaling on simulated river discharge. Environ. Earth Sci. 71 (11), 4849–4868. https://doi.org/10.1007/s12665-013-2876-z.

Mauser, W., Bach, H., 2009. PROMET – Large scale distributed hydrological modelling to study the impact of climate change on the water flows of mountain watersheds. J. Hydrol. 376 (3), 362–377. https://doi.org/10.1016/j.jhydrol.2009.07.046.

Mauser, W., Klepper, G., Zabel, F., Delzeit, R., Hank, T., Putzenlechner, B., Calzadilla, A., 2015. Global biomass production potentials exceed expected future demand without the need for cropland expansion. Nat. Commun. 6, 8946. https://doi.org/10.1038/ncomms9946.

Muñoz-Sabater, J., et al., 2021. ERA5-Land: a state-of-the-art global reanalysis dataset for land applications. Earth Syst. Sci. Data Discuss. 1–50. https://doi.org/10.5194/essd-2021-82.

Nash, J.E., Sutcliffe, J.V., 1970. River flow forecasting through conceptual models part I — a discussion of principles. J. Hydrol. 10 (3), 282–290. https://doi.org/10.1016/0022-1694(70)90255-6.

Pagliero, L., Bouraoui, F., Willems, P., Diels, J., 2014. Large-scale hydrological simulations using the soil water assessment tool, protocol development, and application in the Danube Basin. J. Environ. Qual. 43 (1), 145–154. https://doi.org/10.2134/jeq2011.0359.

Petrovič, P., Mravcová, K., Holko, L., Kostka, Z., Miklánek, P., 2010. Basin-wide water balance in the Danube River Basin. In: Brilly, M. (Ed.), Hydrological Processes of the Danube River Basin. Springer, Dordrecht, pp. 227–258. 10.1007/978-90-481-3423-6_7.

Prein, A.F., Gobiet, A., 2017. Impacts of uncertainties in European gridded precipitation observations on regional climate analysis. Int. J. Climatol. 37 (1), 305–327. https://doi.org/10.1002/joc.4706.

Sacks, W.J., Deryng, D., Foley, J.A., Ramankutty, N., 2010. Crop planting dates: an analysis of global patterns. Glob. Ecol. Biogeogr. 19 (5), 607–620. https://doi.org/10.1111/j.1466-8238.2010.00551.x.

Schiller, H., Miklós, D., Sass, J., 2010. The Danube River and its basin physical characteristics, water regime and water balance. In: Brilly, M. (Ed.), Hydrological Processes of the Danube River Basin. Springer, Dordrecht, pp. 25–77. https://doi.org/10.1007/978-90-481-3423-6_2.

Schneider, U., Finger, P., Meyer-Christoffer, A., Rustemeier, E., Ziese, M., Becker, A., 2017. Evaluating the hydrological cycle over land using the newly-corrected precipitation climatology from the Global Precipitation Climatology Centre (GPCC). Atmosphere 8 (3), 52. https://doi.org/10.3390/atmos8030052.

Schwarb, M., Daly, C., Frei, C., Schär, C., 2001. Mean annual and seasonal precipitation in the European Alps 1971-1990. Hydrological Atlas of Switzerland. Fed. Off. Environ., Bern.

Sevruk, B., 2005. Rainfall measurement: gauges. In: Anderson, M.G. (Ed.), Encyclopedia of Hydrological Sciences. Part 4 Hydrometeorology. Wiley & Sons Ltd, Chichester, UK, pp. 529–535.

Shrestha, M., Acharya, S.C., Shrestha, P.K., 2017. Bias correction of climate models for hydrological modelling – are simple methods still useful? Meteorol. Appl. 24 (3), 531–539. https://doi.org/10.1002/met.1655.

Stagl, J.C., Hattermann, F.F., 2015. Impacts of climate change on the hydrological regime of the Danube River and its tributaries using an ensemble of climate scenarios. Water 7 (11), 6139–6172. https://doi.org/10.3390/w7116139.

Tarek, M., Brissette, F.P., Arsenault, R., 2020. Evaluation of the ERA5 reanalysis as a potential reference dataset for hydrological modelling over North America. Hydrol. Earth Syst. Sci. 24 (5), 2527–2544. https://doi.org/10.5194/hess-24-2527-2020.

Todini, E., 2007. A mass conservative and water storage consistent variable parameter Muskingum-Cunge approach. Hydrol. Earth Syst. Sci. 11 (5), 1645–1659. https://doi.org/10.5194/hess-11-1645-2007.

Weedon, G.P., Gomes, S., Viterbo, P., Shuttleworth, W.J., Blyth, E., Österle, H., Adam, J.C., Bellouin, N., Boucher, O., Best, M., 2011. Creation of the WATCH forcing data and its use to assess global and regional reference crop evaporation over land during the twentieth century. J. Hydrometeorol. 12 (5), 823–848. https://doi.org/10.1175/2011JHM1369.1.

Yapo, P.O., Gupta, H.V., Sorooshian, S., 1996. Automatic calibration of conceptual rainfall-runoff models: sensitivity to calibration data. J. Hydrol. 181 (1), 23–48. https://doi.org/10.1016/0022-1694(95)02918-4.

Yilmaz, K.K., Vrugt, J.A., Gupta, H.V., Sorooshian, S., 2010. Model calibration in watershed hydrology. In: Sivakumar, B., Berndtsson, R. (Eds.), Advances in Data-Based Approaches for Hydrologic Modeling and Forecasting. World Scientific, Hackensack, NJ, pp. 53–105.

Zabel, F., Putzenlechner, B., Mauser, W., 2014. Global agricultural land resources – a high resolution suitability evaluation and its perspectives until 2100 under climate change conditions. PLoS One 9 (9), e107522. https://doi.org/10.1371/journal.pone.0107522.